Supporting Information for

Microsecond Blinking Events in the Fluorescence of Colloidal Quantum Dots Revealed by Correlation Analysis on Preselected Photons

*Freddy T. Rabouw, Felipe V. Antolinez, Raphael Brechbühler, and David J. Norris**

Optical Materials Engineering Laboratory, Department of Mechanical and Process Engineering, ETH Zurich, 8092 Zurich, Switzerland

* Corresponding author. E-mail: dnorris@ethz.ch

Methods

Samples: CdSe/CdS/ZnS core/shell/shell quantum dots were synthesized following the procedure of Boldt *et al.*[S1] and CdSe/CdS dot-in-rods following the procedure of Coropceanu *et al.*[S2] Figures 1–4 in the main text and Figures S1–3, S5a–e, S8a–h, S9i–p in the Supporting Information show data for CdSe/CdS (8 ML)/ZnS (2 ML) quantum dots, with an ensemble photoluminescence lifetime of 55 ns and quantum yield of 65% in hexane. Figures S7i–p, S8a–h in the Supporting Information show data for CdSe/CdS dot-in-rods.

Spectroscopic experiments: For time-correlated single-photon counting on individual quantum dots, a dilute dispersion of quantum dots in hexane was spin-coated on a glass cover slip to obtain a surface coverage of $\sim 0.1\ \mu m^{-2}$. The sample was loaded on a Nikon Ti-U inverted microscope equipped with a 100× oil-immersion objective (Nikon, CFI Plan Apo VC) with a numerical aperture of 1.4 that was simultaneously used to excite the quantum dots and collect the fluorescence. An individual quantum dot was excited at a repetition rate of 10 MHz and a fluence of $\sim 1\ \mu J\,cm^{-2}$ using a focused 405-nm pulsed laser diode (Picoquant LDH-D-C-405). The quantum-dot fluorescence was sent to a Hanbury-Brown–Twiss setup with a non-polarizing 50/50 beam splitter and two nominally identical Excelitas SPCM-AQRH-14-TR avalanche photodiodes. Photon counts from the detectors and a reference signal from the laser diode were recorded on a Picoquant HydraHarp 400 time-tagging module operated in time-tagged time-resolved mode. Photoluminescence quantum yields were measured at room temperature with excitation at 405 nm, using a Hamamatsu C11347 Quantaurus-QY spectrometer equipped with an integrating sphere. Ensemble photoluminescence decays were measured with an Edinburgh Instruments FLS 980 fluorometer, exciting with a pulsed diode laser at 375 nm with a repetition rate of 1 MHz.

Monte Carlo simulations of blinking: In our Monte Carlo model for blinking we simulated random switching of a quantum dot between a bright ON and a dark OFF state according to the desired statistics as well as optical cycling between the ground state and excited state. The quantum dot was initiated at time $t = 0$ in the ON state and in the ground state. A random duration of the ON state t_{ON} was drawn from a power-law distribution (t^{-p}) with lower limit $t_{min} = 1\ \mu s$, upper limit $t_{max} = 1$ s, exponent p_{ON1} for times < 1 ms, and exponent p_{ON2} for times > 1 ms (see distributions plotted in Figure 4 of the main text). Until a time t_{ON} has passed, the quantum dot cycles between its ground and excited states. When the quantum dot is in the ground state, the time until excitation is drawn from an exponential distribution with mean $t_{exc} = 2.7\ \mu s$. (This value was chosen to obtain simulated count rates similar to those found experimentally.) Next, the time until relaxation to the ground state is drawn from an exponential distribution with mean $t_{rec,ON} = 50$ ns. Upon relaxation, a photon is recorded with probability $\eta_{det} = 10\ \%$. If so, the photon emission time is stored and the quantum dot returns to the ground state. If not, the quantum dot returns to the ground state without a photon detection event. This optical cycling continues until after the first relaxation event at a time exceeding the duration of the ON period $t > t_{ON}$. The quantum dot then transitions to the OFF state. The duration of the OFF state is again drawn from a power-law distribution, but with $t_{max} = 100$ ms, and exponents p_{OFF1} and p_{OFF2}. The OFF state persists until the first relaxation event after the simulated OFF duration ends. Optical cycling in the OFF period again uses the exponential statistics for excitation and relaxation, but with mean relaxation time $t_{rec,OFF} = 7$ ns. The probability that upon relaxation a photon is recorded is reduced to $\eta_{em}\eta_{det} = 2.5\ \%$, where $\eta_{em} = 25\ \%$ accounts for the finite quantum efficiency of the quantum dot in the OFF state. After the OFF state ends, the quantum dot returns to the ON state and the procedure starts from the beginning. Note that if sub-ms blinking is included in the simulation and we then apply binning and thresholding to the simulated photon stream, the statistics of ON and OFF durations extracted are different from the statistics we put in (see Supporting Information Figure S6). The correlation functions of Figure 4 in the main text were obtained from a total simulated experiment time of 6000 s.

Derivation of eq 2 in the main text

We consider the maximum bunching amplitude in the intensity correlation function constructed from preselected photons emitted by an individual quantum dot during time bins with an average emission intensity $\langle I \rangle$. We assume that a timescale t_{max} exists that is faster than the fastest blinking events in the quantum dot, but slower than the excited-state lifetime. Over this short timescale the quantum dot does not switch between ON and OFF states, while still anti-bunching due to single-photon emission does not affect the photon statistics. In this case, $\langle I(t)I(t+t_{max})\rangle = \langle I(t)I(t)\rangle = \langle I^2\rangle$, where $\langle I^2\rangle$ is emission intensity squared averaged over the time bins selected. We then obtain for the expected value of the intensity correlation function $g^{(2)}$ that

$$g^{(2)}(t_{max}) = \frac{\langle I(t)I(t+t_{max})\rangle}{\langle I(t)\rangle\langle I(t+t_{max})\rangle} = \frac{\langle I^2\rangle}{\langle I\rangle^2}. \quad (1)$$

If we consider that the average intensity in the selected time bins is determined by two-state blinking between an ON state with intensity I_{ON} and an OFF state with intensity I_{OFF}, then the average intensity as well as the average intensity squared depend on the fraction of time f that the quantum dot is in the ON state during the time bins selected (see also Figure S4):

$$\langle I\rangle = fI_{ON} + (1-f)I_{OFF}, \quad (2)$$

$$\langle I^2\rangle = fI_{ON}^2 + (1-f)I_{OFF}^2. \quad (3)$$

We can use this to express the maximum bunching amplitudes in terms of the average intensity in the time bins selected and the ON and OFF intensities:

$$g^{(2)}(t_{max}) = \frac{\langle I^2\rangle}{\langle I\rangle^2} = \frac{fI_{ON}^2 + (1-f)I_{OFF}^2}{\langle I\rangle^2} = \frac{I_{ON}\langle I\rangle - (1-f)I_{ON}I_{OFF} + I_{OFF}\langle I\rangle - fI_{ON}I_{OFF}}{\langle I\rangle^2} = \frac{I_{ON}+I_{OFF}}{\langle I\rangle} - \frac{I_{ON}I_{OFF}}{\langle I\rangle^2}. \quad (4)$$

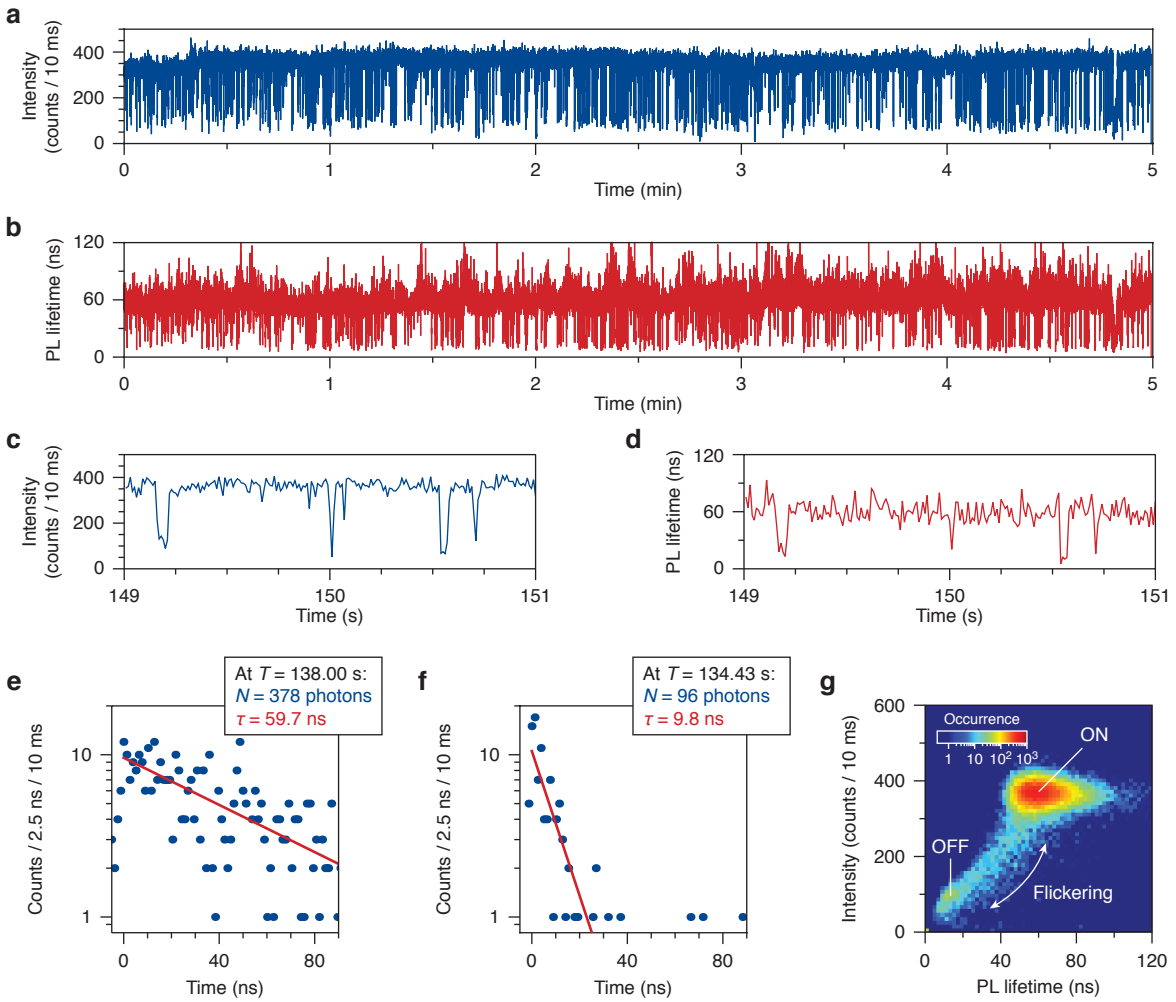

Figure S1 | Lifetime fluctuations and the fluorescence lifetime intensity distribution. **(a)** The full intensity trace of the experiment analyzed in detail in the main text (Figures 1–4), binned at 10 ms, from an individual CdSe (3.2 nm diameter)/CdS (8 ML)/ZnS (2 ML) QD excited at 405 nm with a repetition rate 10 MHz and pulse fluence of 1 μJ cm^{-2}. **(b)** The corresponding photoluminescence (PL) lifetime trace, obtained by fitting the PL decay histogram for each 10-ms time bin using a maximum-likelihood routine,[S3] as shown in panels **e,f**. **(c,d)** Zoom-in of the data in panels **a** and **b**, respectively. **(e)** An example of a PL decay trace, i.e. a histogram of photon arrival times with respect to the laser excitation, recorded during time bin number 13800 that contains 378 photons. The red line is a maximum-likehood fit[S3] to a single-exponential decay [$I(t) = I(0)\mathrm{e}^{-t/\tau}$], yielding a lifetime of $\tau = 59.7$ ns. **(f)** A second example of a PL decay trace for bin number 13443 that contains as few as 96 photons (i.e., the QD is OFF), yielding a lifetime of $\tau = 9.8$ ns. **(g)** The fluorescence lifetime intensity distribution (FLID), a 2-dimensional histogram of the emission intensities and PL lifetimes recorded during the experiment, constructed from the data of panels **a,b**.

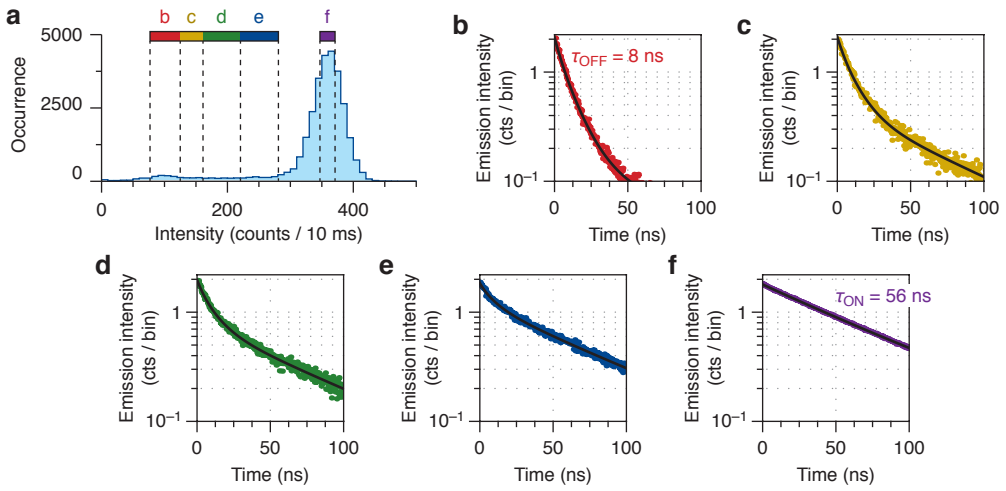

Figure S2 | Blinking by charging/discharging. (a) The intensity histogram of the experiment discussed in detail in the main text (Figures 1–4), with intensity ranges highlighted with colored bars from which photons were selected to construct the PL decay histograms in panels **b–f**. **(b–f)** PL decay curves (data points) at different emission intensities as indicated in panel **a**, at 76–124 (red; **b**), 124–160 (yellow; **c**), 160–220 (green; **d**), 220–280 (blue; **e**), and 348–372 (purple; **f**) counts/10 ms. These are the same selections as made in the main text (Figure 3) to construct correlation functions. The black lines are weighted least-squares fits to a biexponential decay with one global value of $\tau_{ON} = 55.7$ ns for the lifetime of the slow component and one global value of $\tau_{OFF} = 7.9$ ns for the fast component. The PL decay amplitude—with each component corrected for pile-up[†] due to the fast laser repetition rate $1/T$ according to $A \rightarrow A(1 - e^{-T/\tau})$—is higher in the OFF state (**b**) than in the ON state (**f**) by a factor 1.32. This is a signature of blinking by charging/discharging.[S4,S5] The higher PL decay amplitude in the charged state is a result of the increased radiative decay rate.

[†]*Derivation of the pile-up correction:* the photoluminescence decay curve is the decay of the emission signal following a laser pulse. The signal following laser pulse i is due to the excited-state population generated by pulse i plus the population generated by pulses $i-1$, $i-2$, etc. Neglecting saturation effects, the total signal is therefore $I(t) = Ae^{-t/\tau} + Ae^{-(t+T)/\tau} + Ae^{-(t+2T)/\tau} + \ldots$. This is a geometric series that can be written as $I(t) = \dfrac{Ae^{-t/\tau}}{1 - e^{-T/\tau}}$. Hence the apparent amplitude of the decay curve must be multiplied by $(1 - e^{-T/\tau})$ to get the photoluminescence decay amplitude A due to the excited-state population generated by an individual laser pulse.

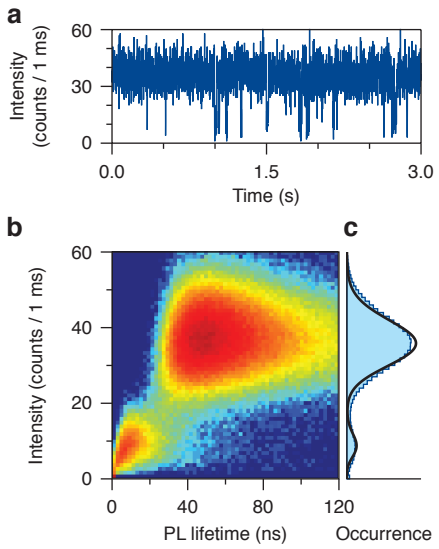

Figure S3 | Binning with a time resolution of 1 ms. **(a)** The same data as plotted in Figures 1a,e of the main text, but using 1-ms time binning. **(b)** The corresponding fluorescence lifetime intensity distribution. The peaks ascribed to the ON and OFF states are broader (relative to the mean values) than with 3-ms or 10-ms time binning (Figures 1b,f in the main text), both in the intensity direction because of Poisson noise and in the PL lifetime direction because of increased fit uncertainties. **(c)** The 1-dimensional intensity histogram. The black solid line is a sum of two Poisson distributions centered at $I_{\mathrm{OFF}} = 9.3$ counts/1 ms and $I_{\mathrm{ON}} = 36.4$ counts/1 ms. The tails of the distributions overlap at approximately three standard deviations from the mean, making a proper analysis of blinking statistics by means of thresholding impossible. This problem becomes worse for even finer time binning than 1 ms, thus limiting the possibilities of binning and thresholding to analyze fast blinking dynamics.

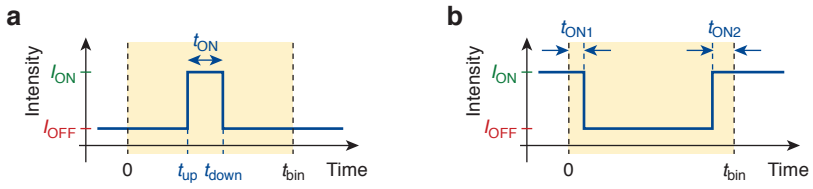

Figure S4 | The intensity correlation function due to a single flickering event. **(a)** Schematic of a time bin within which the QD rapidly flickers OFF → ON → OFF (zoom-in of Figure 4a in the main text). The average intensity during this bin is $\langle I \rangle = fI_{\mathrm{ON}} + (1-f)I_{\mathrm{OFF}}$, where $f = t_{\mathrm{ON}}/t_{\mathrm{bin}}$. For our analytical calculation of $g^{(2)}(\tau) = \dfrac{\langle I(t)I(t+\tau)\rangle}{\langle I(t)\rangle\langle I(t+\tau)\rangle}$ corresponding to bins selected to show an average intensity $\langle I \rangle$, we average over all possible moments $t_{\mathrm{up}} \in [0, t_{\mathrm{bin}}]$ of the ON → OFF switch while keeping f constant. **(b)** Schematic of a rapid ON → OFF → ON flickering event. Our averaging procedure includes these situations, where we keep $t_{\mathrm{ON1}} + t_{\mathrm{ON2}} = t_{\mathrm{ON}}$. The scenario that the time bin contains a single ON–OFF switch is a special case of this situation with $t_{\mathrm{ON1}} = t_{\mathrm{ON}}$. The scenario of a single OFF-ON switch is a special case with $t_{\mathrm{ON2}} = t_{\mathrm{ON}}$. In our simple calculation we do not assign a special (increased) weight to these scenarios in the averaging procedure. In practice, depending on the blinking statistics, this scenario may be more frequent than considered here, but it does not produce a slope in the correlation function on the microsecond timescales like we observe experimentally.

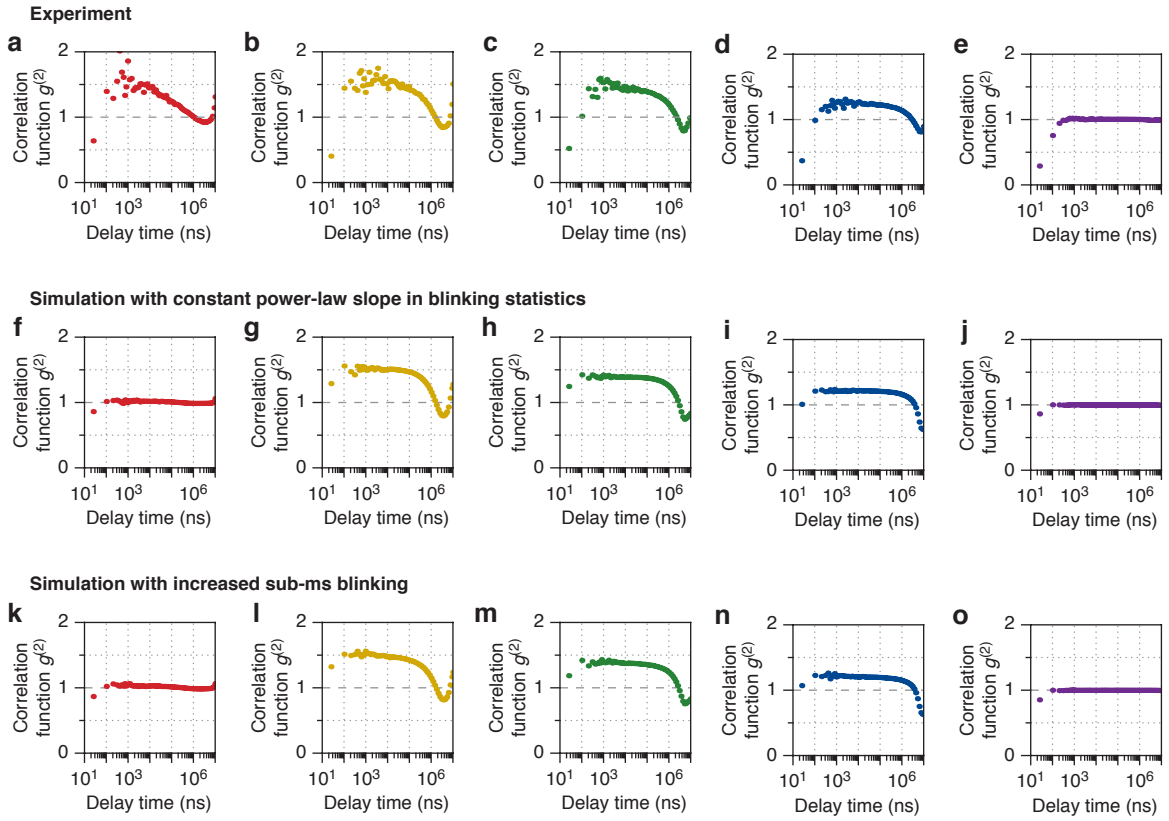

Figure S5 | Correlation analysis on Monte Carlo simulations of quantum-dot blinking. **(a–e)** Data reproduced from Figure 3c–g in the main text: experimental correlation functions on preselected photons, emitted during periods with increasing emission intensity (from **a** to **e**) as color labeled in Figure 3b,h in the main text. **(f–j)** Same, but for simulated data of quantum-dot blinking with statistics as plotted in Figure 4c of the main text, i.e. with $p_{ON1} = p_{ON2} = 1.2$ and $p_{OFF1} = p_{OFF2} = 1.1$. **(k–o)** Same, but for simulated data of quantum-dot blinking with statistics as plotted in Figure 4f of the main text, i.e. with $p_{ON1} = 1.7; p_{ON2} = 1.2$ and $p_{OFF1} = 1.6; p_{OFF2} = 1.1$. The qualitative difference between the simulation results in **f,k** compared to the experimental result in **a** indicates that, as we discuss in the main text, the quantum dot in the experiment has multiple OFF states with low intensity rather than a single well-defined OFF state with emission intensity I_{OFF} as we assume in the simulation.

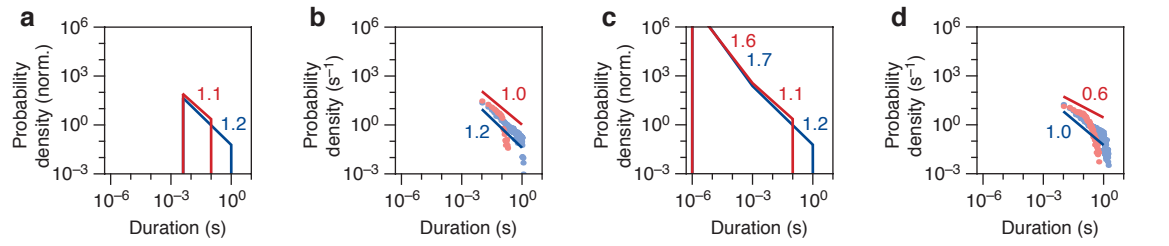

Figure S6 | Blinking statistics from Monte Carlo simulations. **(a)** Input statistics for a Monte Carlo simulation of quantum-dot blinking: $p_{ON} = 1.2$ on the range of 5 ms $< t_{ON} <$ 1 s and $p_{OFF} = 1.1$ on the range of 5 ms $< t_{ON} <$ 100 s without any sub-ms blinking. **(b)** Blinking statistics extracted from this simulation by 10-ms binning and thresholding, recovering the input statistics. **(c)** Input statistics for the Monte Carlo simulation of quantum-dot blinking discussed in the main text (Figure 4f–h): $p_{ON1} = 1.2; p_{ON2} = 1.7; p_{OFF1} = 1.1; p_{OFF2} = 1.6$. **(d)** Blinking statistics extracted from this simulation by 10-ms binning and thresholding, yielding power-law slopes deviating from the input due to flickering on sub-binning timescales.

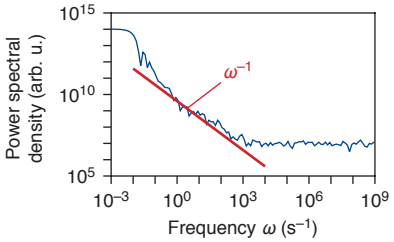

Figure S7 | Power spectral density analysis of blinking, inspired by ref S6. Power spectrum of the intensity trace (Figure 1a,e in the main text) of the individual CdSe/CdS/ZnS quantum dot analyzed in detail in the main text. Specifically, we Fourier transform the intensity trace

$$y(t) = \sum_{i}^{\text{photons}} \delta(t - t_i),$$

where $\delta(x)$ is the Dirac delta function and t_i is the time stamp of photon detection event, into

$$\hat{y}(\omega) = \int y(t) \mathrm{e}^{-\omega t} \, \mathrm{d}t = \sum_{i}^{\text{photons}} \mathrm{e}^{-\omega t_i}.$$

The plot shows the power spectral density $|\hat{y}(\omega)|^2$ as a function of frequency ω. The plot is smoothened by averaging $|\hat{y}(\omega)|^2$ over 10 evaluations at consecutive values of ω on a logarithmic grid. We observe finite-size artifacts at low frequencies $\omega < 10^{-2}\ \mathrm{s}^{-1}$ of the order of the inverse experiment time, then an approximate ω^{-1} slope on the interval $10^{-2}\ \mathrm{s}^{-1} < \omega < 10^{3}\ \mathrm{s}^{-1}$ (red dashed line), followed by a flat background for frequencies $\omega > 10^{3}\ \mathrm{s}^{-1}$ of the order of the count rate and higher. Other quantum dots show qualitatively similar power spectral density functions.

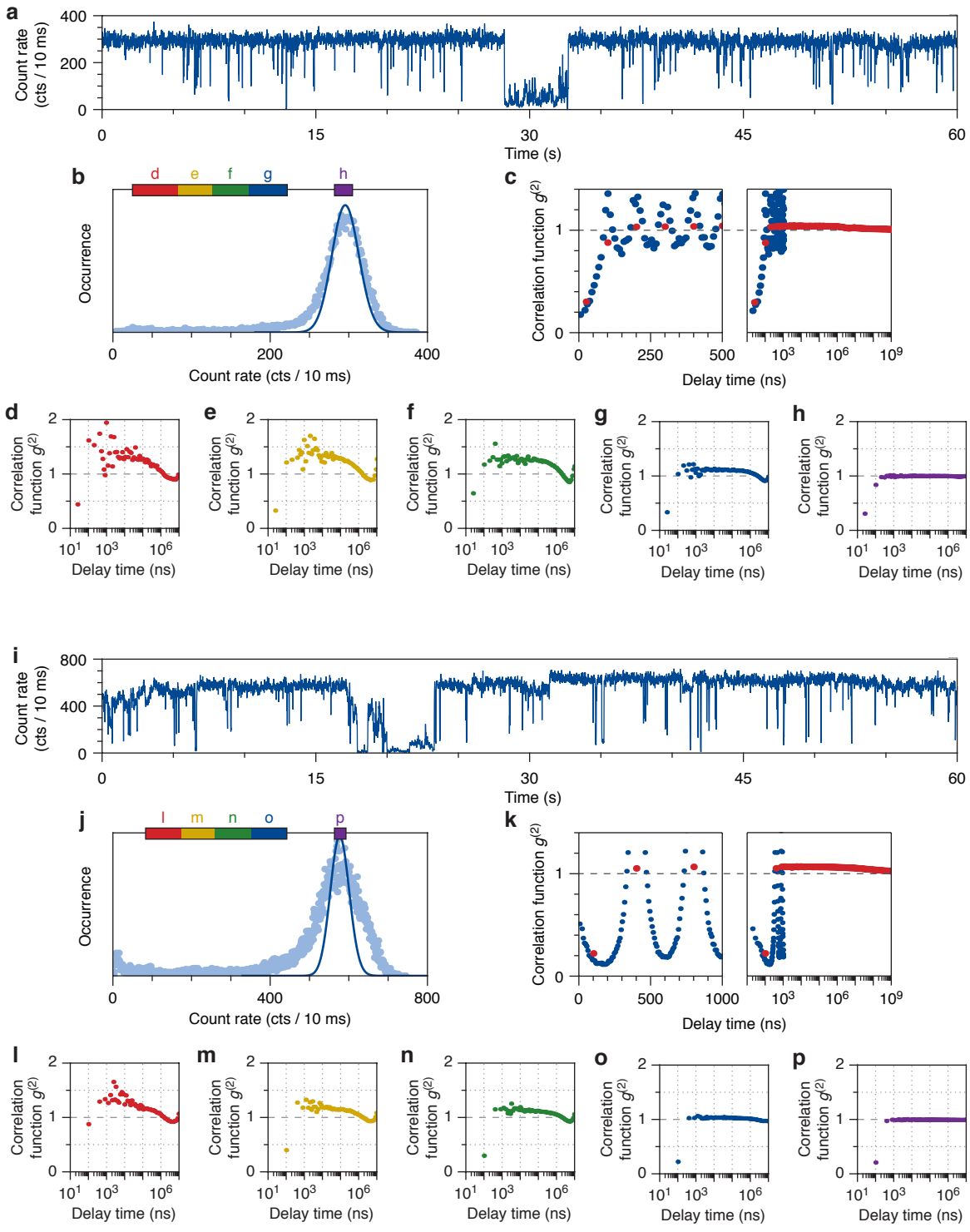

Figure S8 | More examples of quantum emitters showing microsecond blinking. **(a–h)** Data for a CdSe/CdS/ZnS quantum dot: **(a)** the intensity trace at 10-ms binning, **(b)** the corresponding intensity histogram, **(c)** the intensity correlation function for the full experiment, and **(d–h)** correlation functions constructed for preselected photons based on the counts in a 10-ms bin, following the criteria as labeled in panel **b**. The correlation functions at intermediate intensities (panels **d–g**) show clear signatures of sub-millisecond blinking. **(i–p)** Same, but for a CdSe/CdS dot-in-rod.

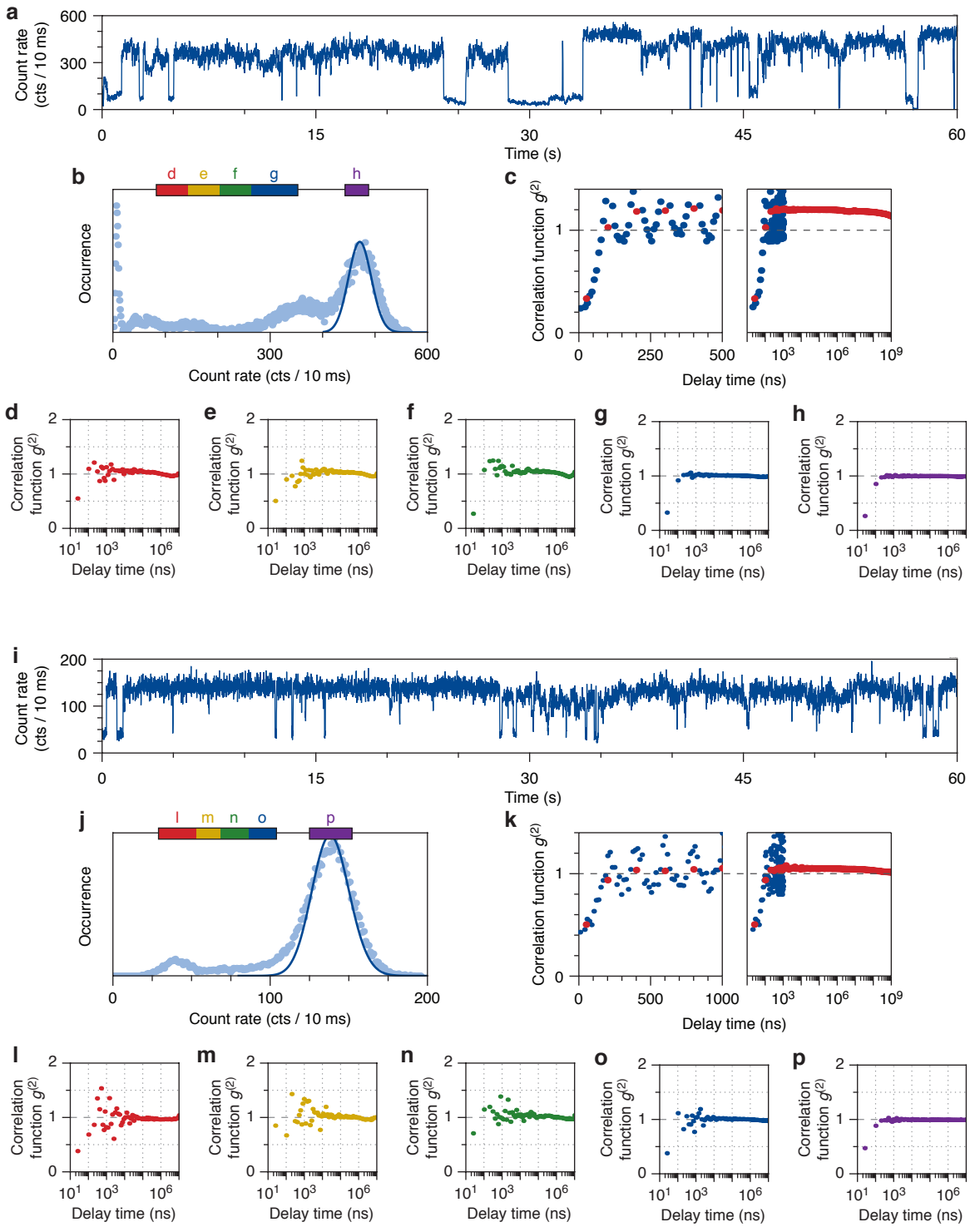

Figure S9 | Examples of quantum emitters showing intermediate-intensity states. (a–h) Data for a CdSe/CdS dot-in-rod: **(a)** the intensity trace at 10-ms binning, **(b)** the corresponding intensity histogram, **(c)** the intensity correlation function for the full experiment, and **(d–h)** correlation functions constructed for preselected photons based on the counts in a 10-ms bin, following the criteria as labeled in panel **b**. The intensity histogram (panel **b**) shows intermediate-intensity states. And indeed, the correlation functions at intermediate intensities (panels **d–g**) are now flat, demonstrating that the intermediate intensities are *not* primarily due to flickering on sub-binning timescales. **(i–p)** Same, but for a CdSe/CdS/ZnS quantum dot. The correlation functions at intermediate intensities (panels **l–o**) are consistent not with flickering but with the existence of intermediate-intensity states, although these are not directly in the intensity histogram (panel **j**).

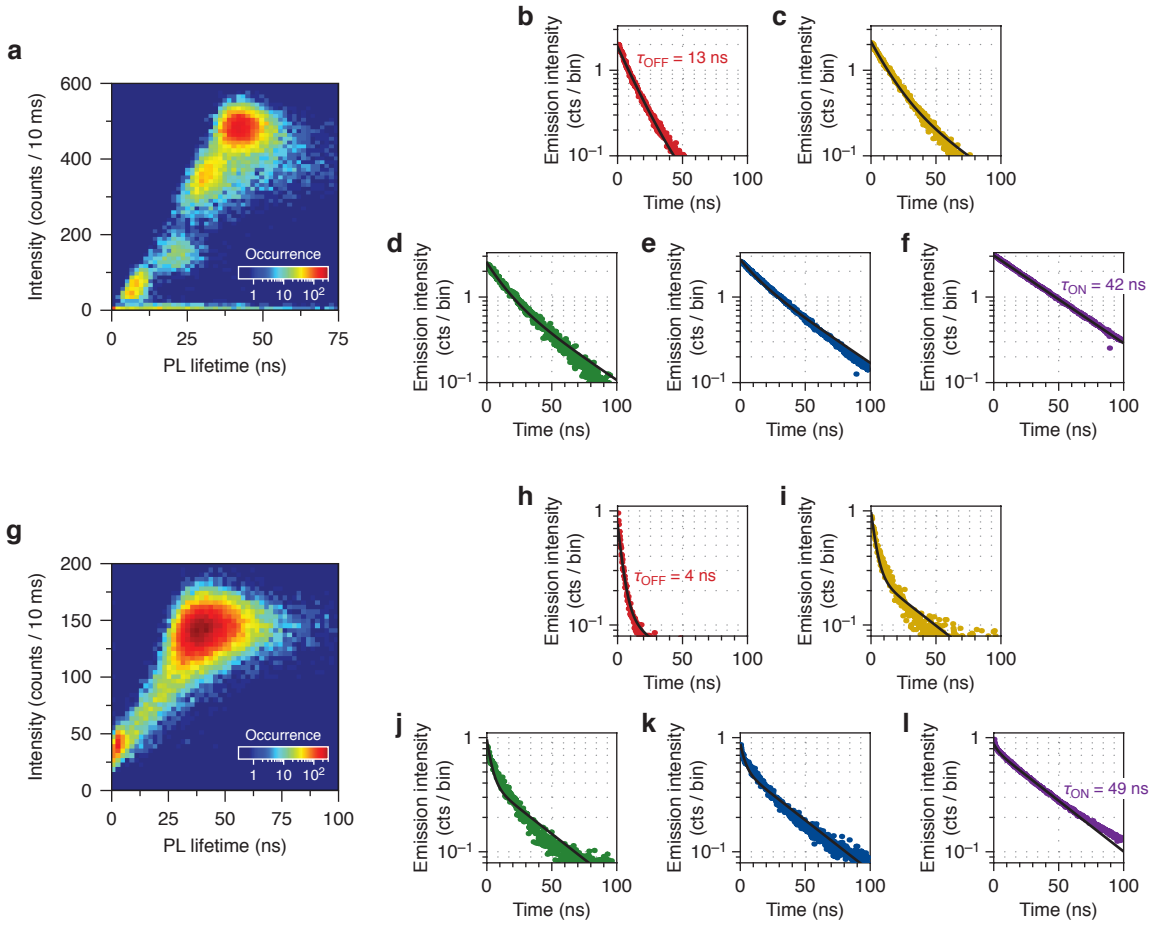

Figure S10 | Lifetime fluctuations of quantum emitters with intermediate-intensity states. **(a)** Fluorescence lifetime intensity distribution of the CdSe/CdS dot-in-rod from Figure S9a–h, with the emission intensity binned at 10 ms and the photoluminescence lifetime fitted with a maximum-likelihood routine[S3] (compare Figure S1). (**b–f**) Photoluminescence decay histograms constructed from photons selected based on the emission intensity in a 10-ms bin, with increasing intensity going from panel **b** to **f** (see color labels in Figure S9b). Black lines are biexponential fits with fixed lifetime components of $\tau_{ON} = 42$ ns and $\tau_{OFF} = 13$ ns. These biexponential fits do not match well with the photoluminescence decay curves of the intermediate intensities (panels **c–e**), consistent with intermediate-intensity states with distinct lifetimes rather than rapid ON–OFF flickering. (**g–l**) Same, but for the CdSe/CdS/ZnS quantum dot from Figure S9i–l. The lifetime components of are $\tau_{ON} = 49$ ns and $\tau_{OFF} = 4$ ns.

Supporting References

(S1) Boldt, K.; Kirkwood, N.; Beane, G. A.; Mulvaney, P. Synthesis of Highly Luminescent and Photo-Stable, Graded Shell CdSe/$Cd_xZn_{1-x}S$ Nanoparticles by In Situ Alloying, *Chem. Mater.* **2013**, *25*, 4731–4738.

(S2) Coropceanu, I.; Rossinelli, A.; Caram, J. R.; Freyria, F. S.; Bawendi, M. G. Slow-Injection Growth of Seeded CdSe/CdS Nanorods with Unity Fluorescence Quantum Yield and Complete Shell to Core Energy Transfer, *ACS Nano* **2016**, *10*, 3295–3301.

(S3) Bajzer, Z.; Therneau, T. M.; Sharp, T. C.; Prendergast, F. G. Maximum Likelihood Method for the Analysis of Time-Resolved Fluorescence Decay Curves, *Eur. Biophys. J.* **1991**, *20*, 247–262.

(S4) Galland, C.; Ghosh, Y.; Steinbrück, A.; Hollingsworth, J. A.; Htoon, H.; Klimov, V. I. Lifetime Blinking in Nonblinking Nanocrystal Quantum Dots. *Nat. Commun.* **2012**, *3*, 908.

(S5) Hiroshige, N.; Ihara, T.; Saruyama, M.; Teranishi, T.; Kanemitsu, Y. Coulomb-Enhanced Radiative Recombination of Biexcitons in Single Giant-Shell CdSe/CdS Core/Shell Nanocrystals. *J. Phys. Chem. Lett.* **2017**, *8*, 1961–1966.

(S6) Pelton, M.; Smith, G.; Scherer, N. F.; Marcus, R. A. Evidence for a Diffusion-Controlled Mechanism for Fluorescence Blinking of Colloidal Quantum Dots. *Proc. Natl. Acad. Sci.* **2007**, *104*, 14249–14254.